

LETTER

A simple approach to analyze layer-dependent optical properties of few-layer transition metal dichalcogenide thin films

To cite this article: Asma Alkabsh *et al* 2019 *Nanotechnology* **30** 03LT02

View the [article online](#) for updates and enhancements.



IOP | ebooks™

Bringing you innovative digital publishing with leading voices to create your essential collection of books in STEM research.

Start exploring the [collection](#) - download the first chapter of every title for free.

Letter

A simple approach to analyze layer-dependent optical properties of few-layer transition metal dichalcogenide thin films

Asma Alkabsh , Hassana Samassekou and Dipanjan Mazumdar¹

Physics Department, 1245 Lincoln Drive, Southern Illinois University, Carbondale, IL 62901 United States of America

E-mail: asma-alkabsh@hotmail.com and dmazumdar@siu.edu

Received 5 September 2018, revised 11 October 2018

Accepted for publication 24 October 2018

Published 12 November 2018



CrossMark

Abstract

Intense interest in transition metal dichalcogenides (TMDs) is driven, among other things, by their intriguing layer-dependent optical properties down to the monolayer and strong excitonic effects. Experimental determination of optical constants such as the complex refractive index and dielectric function of large-area TMDs thin films is prone to large uncertainties at the few-layer level using a single measurement technique such as spectroscopic ellipsometry (SE). In this work, we demonstrate an approach to accurately determine the optical constants by combining transmission spectroscopy with SE. Using MoS₂ as an example, the prototypical TMD material, we demonstrate our approach on transparent (Quartz, Al₂O₃) and absorbing (e.g. Si/SiO₂) substrates. We find that pre-characterized optical properties from transmission spectroscopy significantly improve the quantitative accuracy of optical constants obtained using SE on both transparent and absorbing substrates. We show that the extracted optical constants from samples deposited on transparent substrates are highly reliable in obtaining layer-dependent optical properties of TMDs while data on absorbing Si/SiO₂ substrate suffer from strong substrate contribution. Overall, we strongly conclude that SE must be combined with transmission spectroscopy to obtain optical constants with high quantitative accuracy. Our approach, though demonstrated on few-layer films, will be applicable to monolayer and bilayer TMDs.

Supplementary material for this article is available [online](#)

Keywords: transition metal dichalcogenides, thin films, optical spectroscopy

(Some figures may appear in colour only in the online journal)

Introduction

Transition metal dichalcogenides (TMDs) have demonstrated a variety of interesting light-matter interactions since the observation of direct gap in monolayer MoS₂ [1]. Such atomically thin materials show strong optical absorption [2] down to the monolayer due to band nesting effect [3] and strong excitonic effects due to strong Coulomb interaction

and spin-orbit effects [4, 5]. Since the discovery of MoS₂, several other TMDs such as MoSe₂, WSe₂ have also shown similar properties [6].

With the development of large-area growth methods using various techniques such as CVD [7–12], MBE [13], PLD [14], and sputtering [15, 16], the estimation of their optical properties pose a different set of challenges compared to exfoliated samples. The distinguishing feature of large-area thin films is the film-substrate interaction and its effect on the optical properties is a relevant topic of interest. An accurate

¹ Author to whom any correspondence should be addressed.

measurement process, including modeling, must provide reliable results regardless of substrate, film thickness, and photon energies.

Choice of substrate depends on the application. Most electronic and opto-electronic applications are based on Si/SiO₂ substrate and all new materials such as few-layer TMDs must be compatible with Silicon to be desirable. However, analysis of optical properties is difficult on absorbing Si which has a band gap of 1.1 eV [17] that strongly overlaps with the fundamental band gap and other relevant optical properties of most TMD semiconductors. For solar-cell and photo-voltaic applications, optical properties on transparent substrates are more relevant. Apart from the substrate effect, understanding the variation of optical properties (such as absorption) with thickness (number of layers) is fundamentally important for TMDs due to its changing band structure. Estimation of thickness dependent optical properties (scaling properties) can be challenging, particularly at the ultra-thin few-layer level.

Popular techniques for analyzing optical properties such as complex dielectric function (ϵ_1 , ϵ_2) and refractive index (n , k) of large-area thin films can be classified either as reflectance-based (e.g. spectroscopic ellipsometry (SE), near-normal reflectance spectroscopy, etc), or transmittance-based (absorption spectroscopy). Both methods have been employed to investigate the properties of TMD materials such as WS₂ [8, 18, 19], MoSe₂, WSe₂ [2, 20, 21], and MoS₂ [22–27]. With photo-excitation, TMDs show several excitonic peaks in the 1–3 eV range. Most notable are the A and B excitons that are associated with transitions at the K and K' point of the Brillouin zone [2, 18, 21, 22]. For MoS₂, the A and the B excitons appear near 1.9 eV, with a nearly 200 meV splitting, and do not show strong thickness dependence [2]. A third strong C exciton peak is also observed between 2.6 and 2.9 eV, depending on thickness [23].

It is noteworthy that the most accurate reports of dielectric properties that correctly model all excitonic peaks are on films deposited on transparent substrates such as Quartz and Al₂O₃ (Sapphire) [12, 25, 28, 29]. It is substantially more difficult to analyze data on highly absorbing substrates such as Si/SiO₂ [30]. In particular, the splitting of the A and B excitons may be missed completely due to the strong Si substrate contribution [24, 26, 31, 32]. Yim *et al* show only a single peak at around 2 eV apart from the large C exciton peak at 2.7 eV [24] for MoS₂ on Si/SiO₂ even though the absorbance spectrum on transparent quartz substrate show both the A and the B exciton [24]. This discrepancy is not related to intrinsic material property but due to the film-substrate combination and difficulties originating in modeling such data. It is equally challenging to investigate the scaling behavior of optical properties as a function of thickness. The variation of band gap and photoluminescence with layer thickness is well established in TMDs [1]. But there are only a few reports on optical properties of large-area thin films [23, 24, 29]. With the possible discovery of several new 2D materials in the future, it is of utmost importance to experimentally measure optical constants with high accuracy at any thickness level.

In this paper, we outline and demonstrate a systematic and simple approach of analyzing optical properties of semiconducting TMD films deposited on transparent and absorbing substrates. Using, MoS₂ as an example, we show that it is important to first analyze the properties using transmittance spectroscopy before modeling the data on absorbing substrates like Si/SiO₂. Specifically, we assert that a transmission spectroscopy measurement is an essential first step, and possibly sufficient to estimate complex optical constants of few-layer TMDs. Another equally important conclusion of our study is that pre-determination of optical constants using transmission spectroscopy is necessary in improving the analysis of SE data. This is primarily because the error in estimating optical constant values with arbitrary initial parameters is larger in SE than transmission spectroscopy. Such spurious effects impede proper evaluation of optical properties and can cause severe overestimation of dielectric function (or refractive index) values as the thickness is reduced to the few and monolayer level. We show that this indeterminacy can be corrected by using optical constants from a prior transmission measurement on transparent substrates and incorporating it to model the SE data. We shall refer to this procedure as transmission-assisted spectroscopic ellipsometry (TASE). Following this procedure, we obtain the correct scaling behavior as a function of layer thickness and reliably uncover weak optical features such as A–B excitons on absorbing substrates. We anticipate that our method will be more important for mono and bilayer films as the quantitative errors are much larger as the thickness is reduced using the standard ellipsometry method.

Experimental details

High quality MoS₂ films of various thickness are grown on transparent Quartz (single or double side polished depending on measurements), Al₂O₃ (sapphire), and absorbing Si/SiO₂ by a two-step hybrid process. First, MoS₂ thin films are deposited using magnetron sputtering and then annealed at 700 °C in sulfur environment through Argon flow. The crystal structure and various properties of few-layer MoS₂ films were assessed using x-ray diffraction, UVVIS spectroscopy, Raman spectroscopy and transport. Details about growth and characterization of the films is reported elsewhere [33].

Both SE and transmission spectroscopy measurements were performed in this work. SE measurements were performed from 1.2 to 3.2 eV in steps of 0.01 eV and 70° angle of incidence (J A Wollam M2000V). The three-phase model consisting of the substrate (Quartz/Si/SiO₂), thin film (MoS₂), and ambient (air) was employed to extract the dielectric function and refractive index of MoS₂. Ellipsometry measures the complex reflectance ratio, $\tilde{\rho} = \frac{r_p}{r_s}$, which is parameterized into a real and imaginary part (Ψ and Δ). The ellipsometric equation of the three-phase structure (air, film, substrate) can be written as [34]:

$$\tilde{\rho} = \frac{r_p}{r_s} = \tan \Psi e^{i\Delta} = f(\epsilon_{\text{air}}, \epsilon_{\text{MoS}_2}, \epsilon_{\text{Sub}}, d_{\text{MoS}_2}, \phi, \lambda).$$

The known parameters in this equation are the dielectric function of air (ϵ_{air}), the angle of incidence (ϕ), and wavelength (λ) in addition to the dielectric function of the substrate (ϵ_{Sub}) that is measured and modeled separately. The only unknown parameters are the real and imaginary parts of the complex dielectric function of MoS₂, ϵ_{MoS_2} . The thickness of MoS₂ is estimated from prior growth calibration and inserted as a parameter. Therefore, with two measurable parameters Ψ and Δ , the real and imaginary parts of dielectric function ϵ_1 and ϵ_2 (or refractive index n and extinction coefficient k where $\epsilon_1 = n^2 - k^2$ and $\epsilon_2 = 2nk$) can be extracted [34, 35] by modeling the optical constants with empirical functions. Tauc-Lorentz (T-L) oscillator model [36, 37] is popularly used to describe the optical behavior of semiconductor materials which constrains the allowed absorption to above band gap values. The imaginary part is given by

$$\epsilon_2(E) = \frac{A_{TL} \Gamma E_0}{(E^2 - E_0^2)^2 + E^2 \Gamma^2} \frac{(E - E_g)^2}{E} E > E_g$$

$$= 0 \quad E \leq E_g,$$

where A_{TL} , Γ , E_0 , and E_g are oscillator amplitude, broadening, the central band transition, and Tauc gap respectively in units of eV. The modeled Ψ^{mod} and Δ^{mod} are fitted to experimental parameters and data to achieve a fit based on minimizing the mean-squared-value (MSE) [34, 35] given by

$$\text{MSE} = \frac{1}{2N - M} \sum_{i=1}^N \left[\left(\frac{\Psi_i^{mod} - \Psi_i^{\text{exp}}}{\sigma_{\Psi_j}^{\text{exp}}} \right)^2 + \left(\frac{\Delta_i^{mod} - \Delta_i^{\text{exp}}}{\sigma_{\Delta_j}^{\text{exp}}} \right)^2 \right],$$

where N is the number of measured Ψ and Δ pairs that is included in the fit and M is the number of fit parameters. $\sigma_{\Delta_j}^{\text{exp}}$ represents the standard deviations that will be calculated from the known error bars on the calibration parameters. When best fit is achieved, ϵ_1 is calculated from ϵ_2 using Kramers–Kronig relation as follows

$$\epsilon_1(E) = \epsilon_1(\infty) + \frac{2}{\pi} P \int_{E_g}^{\infty} \frac{E' \epsilon_2(E') - 1}{E'^2 - E^2} dE',$$

where P stands for the Cauchy principal part of the integral [38, 39]. The T-L models were implemented using the WVASE32 software [35].

Transmittance measurement were performed at normal incidence from 1.2 to 3.2 eV in steps of 0.07 eV using the ellipsometer in transmittance mode and separately using a grating spectrometer (Shimadzu UV3600 plus). Both equipment gave nearly identical results. The transmittance equation for the three-phase system is written as [35, 34]

$$t_{total} = \frac{t_{01} t_{12} e^{-i\beta}}{1 + r_{01} r_{12} e^{-2i\beta}},$$

where $t_{01} = \frac{2}{1 + N_1}$, $t_{12} = \frac{2N_1}{N_2 + N_1}$, $r_{01} = \frac{1 - N_1}{1 + N_1}$, $r_{12} = \frac{N_1 - N_2}{N_1 + N_2}$, and $\beta = \frac{2\pi d N_1}{\lambda}$.

The indices 0, 1, and 2 represent the medium of air, film, and substrate respectively. Assuming that N_2 is known and obtained previously, the measured transmittance, t , will be function of N_1 and d which represent MoS₂ film's complex refractive index and thickness respectively.

$$t_{total} = t(n_1, k_1, d).$$

The spectral dependence of t is fitted using T-L model to extract the optical constants. The film thickness is also optimized. The goodness of the fit (MSE) in this case is

$$\text{MSE} = \frac{1}{N_T - M} \sum_{i=1}^{N_T} \left(\frac{T_i^{mod} - T_i^{\text{exp}}}{w_T \sigma_{T_j}^{\text{exp}}} \right)^2,$$

where N_T is the number of experimental intensity transmittance measurements and w_T is the weighting ratio for transmission data which is typically set to one (100%).

Results and discussion

In figures 1(a) and (b), we show the SE data (ψ , Δ) of a bare Si/SiO₂ (100 nm) substrate and a 12 nm MoS₂ film deposited on Si/SiO₂. The 1–3.2 eV range covers the essential characteristics of MoS₂ [23, 24, 29] as described earlier. A casual inspection of the (ψ , Δ) curves reveals the overwhelming contribution of the substrate both qualitatively and quantitatively. The A–B exciton, highlighted by the dashed lines at near 1.8 and 1.9 eV, appear as small peaks on the curves. The C exciton is not obvious on simple visual inspection. Such observations highlight the difficulty in modeling optical constants on absorbing substrates.

The SE data on transparent substrates are substantially different and shown in figures 1(c) and (d). Compared to the film + substrate combination (figure 1(d)), the variation in (ψ , Δ) values of the substrate (figure 1(c)) is relatively small and, as a result, the exciton peaks are relatively prominent. The variation of both ψ and Δ is about 0.5° for the substrate whereas for the film-substrate combination, the variation of ψ is about 6° and over 100° for Δ . This strongly hints that the data on transparent substrates might be easier to analyze, in principle, for accurate determination of optical constants. Data on Al₂O₃ substrate was also qualitatively similar to Quartz and shown in figure S1 is available online at stacks.iop.org/NANO/30/03LT02/mmedia (see supplementary data).

The data is more straightforward in a transmission measurement. In figures 1(e)–(f) we show the transmittance data of the Quartz substrate and a 12 nm MoS₂ film on Quartz. We clearly notice that the excitonic peaks are, at least, as prominent as in ellipsometry (figure 1(d)) with the added advantage of being simpler and intuitive in its interpretation. Therefore, it is reasonable to assert that the analysis of transmission data is probably the simplest and an excellent starting point for accurate determination of optical constants.

The rationale of our approach is as follows. Since T-L model is employed to fit the experimental SE data, a set of arbitrary initial values are required to set up the oscillators during the fit. The arbitrariness, as we show here, can lead to

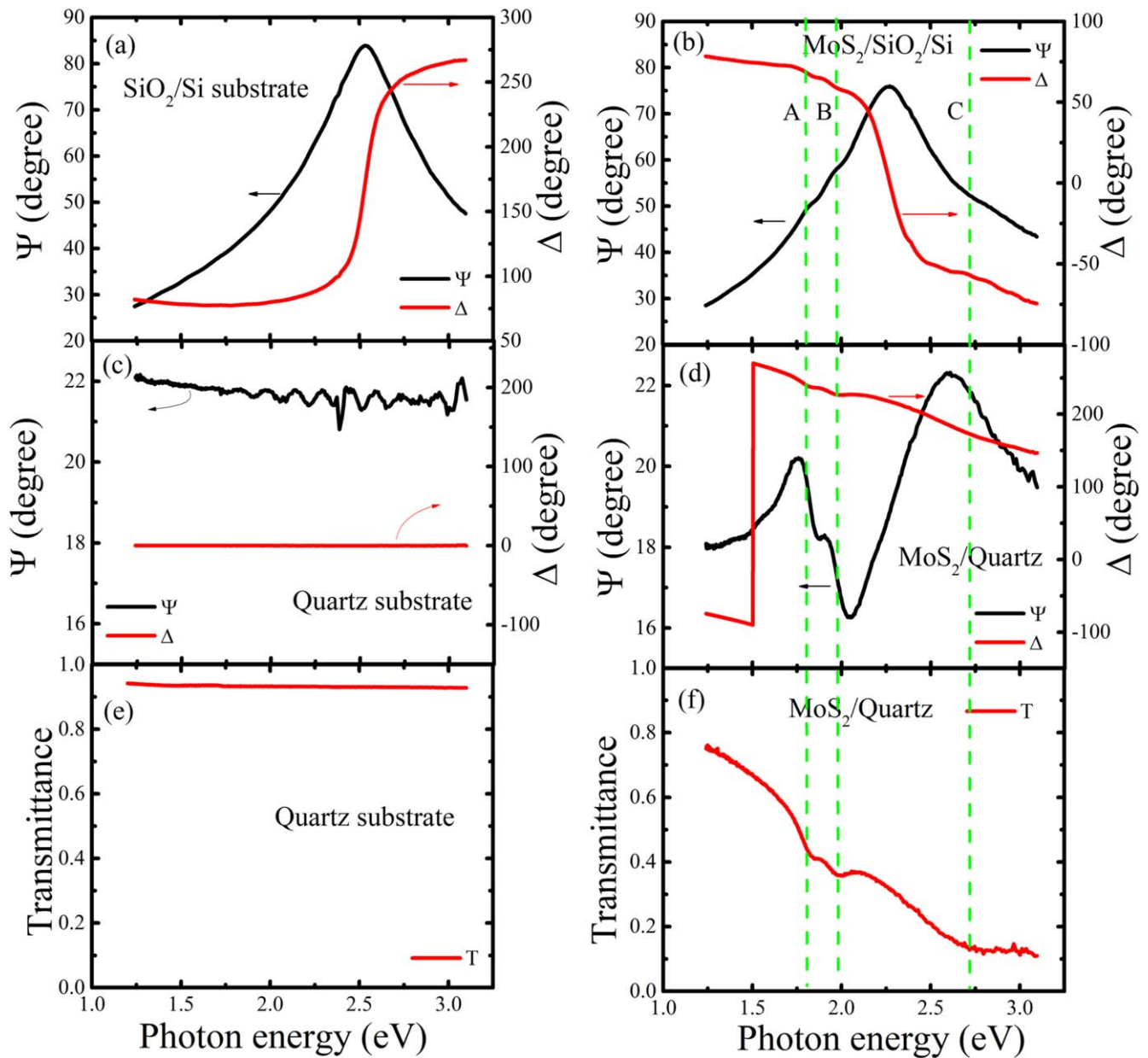


Figure 1. Spectroscopic ellipsometry data of (a) Si/SiO₂ substrate (b) MoS₂ film on Si/SiO₂ (c) Quartz substrate (d) MoS₂ film on Quartz. Transmittance data of (e) Quartz (f) MoS₂ on Quartz. The thickness of the MoS₂ films shown here are between 10 and 12 nm.

large errors in the estimation of optical constants values, apart from possibly missing important optical features. Therefore, obtaining a low MSE value is not a good indicator of the accuracy. Our hypothesis is that the error of modeling with arbitrary initial parameters is much lower when applied to transmittance than the complex reflectance ratio of SE. Moreover, transmission measurements are inherently less prone to misalignment errors than reflectance and less sensitive to surface roughness. While SE measurements on transparent substrates can be accomplished easily, we find that prior characterization of optical constants using transmission spectroscopy can substantially improve the quantitative accuracy of optical constants obtained from SE on transparent substrates. Our general prescription is, therefore, to measure

spectroscopic properties on transparent substrates before proceeding to ellipsometry.

Analysis of normal transmittance on transparent substrates using T-L Model

Transmittance measurements are suitable for weakly absorbing films on transparent substrates. The transmittance data for the MoS₂ film shown in figures 1(e) and (f) was fitted with four T-L oscillators starting with arbitrary initial parameters (apart from the thickness, which was initialized using pre-calibrated values and allowed to vary), one for each A, B and C exciton. A fourth oscillator was also necessary near 3.0 eV that is sometimes referred to as the D peak in the literature [23, 26, 32]. The fit

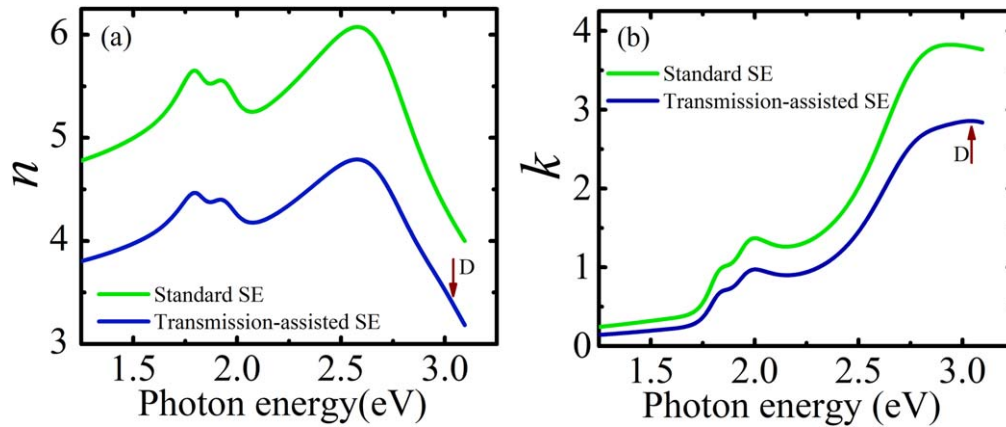


Figure 2. Comparison of (a) refractive index, n , (b) extinction coefficient, k , of a 4L MoS₂ film on quartz substrate using standard ellipsometry (green) and transmission-assisted spectroscopic ellipsometry (blue). Apart from large quantitative differences in both n and k estimation, the D peak is identified at 3.04 eV (dark red arrow) in TASE method only.

Table 1. The modeled T-L oscillators and thickness for a nominally 4L (2.5 nm) sample of MoS₂ on Quartz obtained from transmission spectroscopy, standard SE, and transmission-assisted SE. Oscillator A, B, C, D are peaks that are associated with MoS₂ and TL₁, TL₂, TL₃ are oscillators that are associated with the background. Fitted thickness across all methods was within 0.2nm of the nominal value.

Sample	Data type	Oscillator	A eV	E_0 eV	Γ eV	E_g eV	ϵ_∞	MSE
MoS ₂ /Quartz	Transmission spectroscopy (arbitrary initial parameters)	A	6.40	1.85	0.202	1.186	1.18	0.90
		B	227.6	1.92	0.176	1.85		
		C	21.90	2.72	0.553	1.20		
		D	29.42	3.07	0.965	1.21		
	Standard SE (arbitrary initial parameters)	A	16.45	1.811	0.137	1.52	1.2	1.9
		B	60.00	1.94	0.27	1.66		
		C	102.13	2.72	0.714	1.74		
		TL ₁	21.88	3.94	2.96	0.0001		
	Transmission-assisted SE	TL ₂	25.13	6.87	0.630	0.03	1.3	1.7
		A	33.04	1.815	0.149	1.6		
		B	82.31	1.94	0.193	1.78		
		C	10.75	2.73	0.524	0.45		
		D	5.18	3.04	0.60	0.0001		
		TL ₃	28.78	4.68	1.92	0.0001		

parameters are shown in table 1. Apart from the relative ease of the fit process, a very low MSE value was obtained. Also, the fit thickness was close to the initial value. Therefore, as we hypothesized, transmission spectroscopy is an excellent starting point for analyzing the more complicated SE data.

TASE on transparent substrates

In TASE, we use the fitted optical constants from transmission spectroscopy to initialize the modeling of the SE data on transparent substrates. Table 1 shows the final fit parameters of this procedure along with the fit obtained using arbitrary initial parameters in standard ellipsometry. Even though there is practically no difference in the thickness and MSE values between the methods, the peak assignments and optical constants values show significant differences. First note that the central energy positions are largely unaffected for the A, B and C excitons between the two methods. However, a peak is assigned at 3.94 eV (outside the range of measurement) in standard SE, whereas it is at 3.04 eV in TASE (the D peak), which agrees with transmission spectroscopy although with a

smaller amplitude. Large differences are observed in the oscillator amplitude between the two methods, particularly for the C exciton which is higher by a factor of nearly 10 in standard ellipsometry compared to TASE. Such variations have a drastic impact on the values of the optical constants.

In figure 2 we plot the complex refractive index values of the 4L (2.5 nm) MoS₂ film on Quartz obtained using standard SE and TASE methods. The large differences in optical constants are clear and SE method consistently shows higher values compared to TASE at all energies. The difference is particularly high for refractive index (n) where it is virtually independent of the photon energy whereas the difference in extinction coefficient (k) values increases with higher photon energies. Also significant is that nearly zero extinction coefficient is obtained below the band gap using the TASE method. The position of the D peak is highlighted in TASE data which is missing in standard SE. Most of the variation in values can be pinpointed to the large oscillator amplitude of the C exciton in standard SE that overwhelms smaller contributions. As shown in figure S2, the standard SE data are

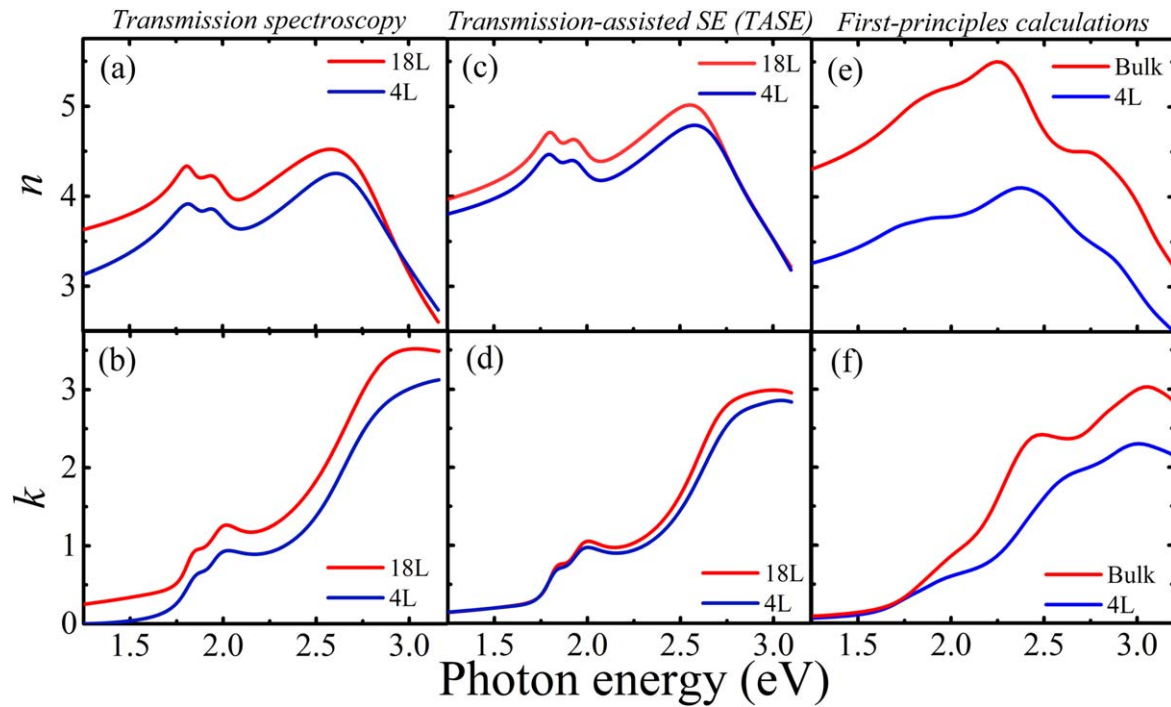


Figure 3. Complex refractive index of a 4L and 18L MoS₂ film obtained using (a)–(b) transmission spectroscopy and (c)–(d) transmission-assisted spectroscopic ellipsometry. (e)–(f) Computed optical constants value using density functional theory of 4L and bulk MoS₂.

also in large discrepancy with theoretical estimates and show inconsistent scaling behavior with thickness.

In figure 3, we compare the extracted optical constants of the 4L and the 18L MoS₂ film on Quartz using the transmission spectroscopy (figures 3(a) and (b)) and the TASE method (figures 3(c) and (d)). The calculated optical constants from density functional theory (DFT) of 4L and bulk MoS₂ are shown in figures 3(e) and (f) using all-electron WIEN2K code [40]. DFT, which describes ground state behavior, cannot describe excitons which are excited states of the system. It is well documented in the literature that the optical constants increase with increasing thickness for TMDs [23–26, 29] as shown in first-principles calculations. Bulk MoS₂ data is shown as it represents the upper bound of the refractive index values. Experimentally, both the scaling behavior with thickness and the quantitative values obtained from transmission and TASE method are in very good agreement with computational results. On the other hand, the scaling behavior obtained from standard SE method is opposite to the trend in figure 3 (see figure S2). Such spurious effects highlight the need to use an additional step in measuring optical properties of ultra-thin films. Compared to TASE, the refractive index value of the 4L film from transmission spectroscopy is slightly lower but in excellent agreement with theory. Also, the extinction coefficient is zero below the band gap for the 4L film and deviates marginally for thicker films. This demonstrates that transmittance data can provide accurate optical properties of few-layer films when combined with Kramers–Kronig consistent T-L modeling. The agreement with theory is even more impressive considering the fact that the experimental measurements are performed on real samples with non-ideal crystal structure, with surface roughness and possibly with a thin surface oxide

layer whereas the theoretical calculations are performed on an ideal crystal structure.

Analysis of data on absorbing substrate implementing TASE method

We next used the optical parameters from TASE as the input for modeling the SE data on other substrates such as absorbing Si/SiO₂ and transparent Al₂O₃. In figure 4, we compare the refractive index values obtained on absorbing Si/SiO₂ along with transparent Quartz and Al₂O₃ substrate for a thick (18L) film. The data on absorbing Si/SiO₂ substrate shows the A, B and C exciton peaks that was directly incorporated during the modeling process. This represent significant improvement compared to other reports [24]. Data on Al₂O₃ show sharper features compared to Quartz with lower broadening energy due to better crystal quality. In table 2, we list the extracted optical parameters of the three samples. While the peak energies and position for the A, B, C excitons are nearly identical on all substrates, the D peak position is particularly clear on Al₂O₃ and not clearly defined on Si/SiO₂ (or possibly blue-shifted outside the range of measurement). Substantially lower refractive index and extinction coefficient values are observed on Si/SiO₂ compared to Quartz/Al₂O₃ even though all films were deposited simultaneously. This can be attributed to the reduced oscillator strengths on absorbing Si/SiO₂ compared to transparent substrates. Since the films are relatively thick (over 10 nm), interface effects should not be major factor and we attribute the effect to strong contribution from the absorbing substrate. In view of such observations, we conclude that thickness dependent scaling behavior are more accurate on transparent

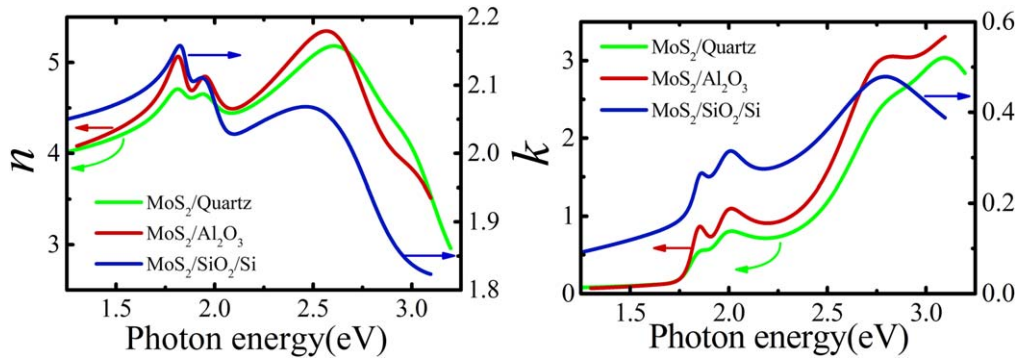


Figure 4. Comparison of extracted optical constants of an 18L MoS₂ film deposited on absorbing (Si/SiO₂) and transparent (Quartz and Al₂O₃) substrates.

Table 2. Modeled T-L oscillator of nominally 12 nm (18L) MoS₂ film deposited on transparent Quartz, Al₂O₃ and Si/SiO₂ using TASE.

Data type	Sample	Oscillator	A eV	E ₀ eV	Γ eV	E _g eV	ε _∞	MSE
Transmission-assisted SE	MoS ₂ /Quartz	A	28.78	1.822	0.132	1.595	1.2	1.9
		B	69.36	1.951	0.194	1.755		
		C	12.25	2.67	0.424	1.18		
		D	16.01	2.97	1.006	0.0001		
	MoS ₂ /Al ₂ O ₃	TL ₁	59.53	4.94	1.973	1.556	1.8	0.89
		A	70.7	1.83	0.10	1.66		
		B	182.7	1.96	0.16	0.15		
		C	36.0	2.69	0.48	0.158		
	MoS ₂ / SiO ₂ /Si	TL ₂	29.7	5.40	1.63	0.158	1.8	5.9
		A	3.92	1.84	0.104	1.67		
		B	2.197	1.985	0.163	1.66		
		C	0.773	2.768	0.655	0.264		
		D	2.387	3.16	3.446	0.0001		
		TL ₃	421.05	3.780	0.564	3.72		

substrates. Therefore, it is convenient to estimate such trends using either a transmission measurement and/or with the TASE method designed here. Our experience shows that this extra effort outweighs the time (apart from accuracy) required to model the data using only standard SE.

In conclusion, we show that the estimation of optical constants of large-area few-layer TMD films on transparent and absorbing substrates using SE can be dramatically improved by pre-characterizing the optical properties using transmission spectroscopy on a transparent substrate. We demonstrate that the designed transmission-assisted SE process improves the reliability of identifying weaker optical features and thickness dependent scaling behavior. Improvements are confirmed on both transparent and absorbing substrates. We also demonstrate that a transmittance measurement in combination with a Kramers–Kronig consistent optical model might be sufficient for accurate estimation of optical constants and scaling behavior of few-layer TMD materials.

Acknowledgments

Dipanjana Mazumdar would like to thank startup funds at Southern Illinois University (SIU). Asma Alkabsh would like to

thank scholarship support from Saudi Arabia Culture Mission. This work used the Extreme Science and Engineering Discovery Environment (XSEDE) which is supported by National Science Foundation grant number ACI-1548562. Computational resources were provided at the San Diego Supercomputer Center (comet) through allocation DMR160135.

ORCID iDs

Asma Alkabsh  <https://orcid.org/0000-0001-5826-2191>

References

- [1] Mak K F, Lee C, Hone J, Shan J and Heinz T F 2010 Atomically thin MoS₂: a new direct-gap semiconductor *Phys. Rev. Lett.* **105** 136805
- [2] Li Y, Chernikov A, Zhang X, Rigosi A, Hill H M, Zande A M V D, Daniel D A, Shih E-M, Hone J and Heinz T F 2014 Measurement of the optical dielectric function of monolayer transition-metal dichalcogenides: MoS₂, MoSe₂, WS₂, and WSe₂ *Phys. Rev. B* **90** 205422

- [3] Carvalho A, Ribeiro R and Neto A C 2013 Band nesting and the optical response of two-dimensional semiconducting transition metal dichalcogenides *Phys. Rev. B* **88** 115205
- [4] Zhang X-X, You Y, Zhao S Y F and Heinz T F 2015 Experimental evidence for dark excitons in monolayer WSe₂ *Phys. Rev. Lett.* **115** 257403
- [5] Zhou Y *et al* 2017 Probing dark excitons in atomically thin semiconductors via near-field coupling to surface plasmon polaritons *Nat. Nanotechnol.* **12** 856
- [6] Manzeli S, Ovchinnikov D, Pasquier D, Yazyev O V and Kis A 2017 2D transition metal dichalcogenides *Nat. Rev. Mater.* **2** 17033
- [7] Dumcenco D, Ovchinnikov D, Sanchez O L, Gillet P, Alexander D T L, Lazar S, Radenovic A and Kis A 2015 Large-area MoS₂ grown using H₂S as the sulphur source *2D Mater.* **2** 044005
- [8] Perea-Lopez N, Elias A L, Berkdemir A, Castro-Beltran A, Gutierrez H R, Feng S, Lv R, Hayashi T, Lopez-Uris F and Ghosh S 2013 Photosensor device based on few-layered WS₂ films *Adv. Funct. Mater.* **23** 5511–7
- [9] Kang K, Xie S, Huang L, Han Y, Huang P Y, Mak K F, Kim C-J, Muller D and Park J 2015 High-mobility three-atom-thick semiconducting films with wafer-scale homogeneity *Nature* **520** 656
- [10] Laskar M R, Ma L, Kannappa S, Park P S, Krishnamoorthy S, Nath D N, Lu W, Wu Y and Rajan S 2013 Large area single crystal (0001) oriented MoS₂ *Appl. Phys. Lett.* **102** 252108
- [11] Shen C-C, Hsu Y-T, Li L-J and Liu S-L 2013 Charge dynamics and electronic structures of monolayer MoS₂ films grown by chemical vapor deposition *Appl. Phys. Express* **6** 125801
- [12] Mitioglu A A, Galkowski K, Surrente A, Klopotoski L, Dumcenco D, Kis A, Maude D K and Plochocka P 2016 Magnetoexcitons in large area CVD-grown monolayer MoS₂ and MoSe₂ on sapphire *Phys. Rev. B* **93** 165412
- [13] Fu D *et al* 2017 Molecular beam epitaxy of highly crystalline monolayer molybdenum disulfide on hexagonal boron nitride *J. Am. Chem. Soc.* **139** 9392–400
- [14] Serna M I, Yoo S H, Moreno S, Xi Y, Oviedo J P, Choi H, Alshareef H N, Kim M J, Minary-Jolandan M and Quevedo-Lopez M A 2016 Large-area deposition of MoS₂ by pulsed laser deposition with *in situ* thickness control *ACS Nano* **10** 6054–61
- [15] Tao J, Chai J, Lu X, Wong L M, Wong T I, Pan J, Xiong Q, Chi D and Wang S 2015 Growth of wafer-scale MoS₂ monolayer by magnetron sputtering *Nanoscale* **7** 2497–503
- [16] Samassekou H *et al* 2017 Viable route towards large-area 2D MoS₂ using magnetron sputtering *2D Mater.* **4** 021002
- [17] Shur M S 1996 *Handbook Series on Semiconductor Parameters* vol 1 (Singapore: World Scientific)
- [18] Zhu B, Chen X and Cui X 2015 Exciton binding energy of monolayer WS₂ *Sci. Rep.* **5** 9218
- [19] Castellanos-Gomez A, Agraït N and Rubio-Bollinger G 2010 Optical identification of atomically thin dichalcogenide crystals *Appl. Phys. Lett.* **96** 213116
- [20] Kravets V G, Prorok V V, Poperenko L V and Shaykevich I A 2017 Ellipsometry and optical spectroscopy of low-dimensional family TMDs *Semicond. Phys., Quantum Electron. Optoelectron.* **20** 284
- [21] Wang K, Huang B, Tian M, Ceballos F, Lin M-W, Mahjouri-Samani M, Boulesbaa A, Poretzky A A, Rouleau C M and Yoon M 2016 Interlayer coupling in twisted WSe₂/WS₂ bilayer heterostructures revealed by optical spectroscopy *ACS Nano* **10** 6612–22
- [22] Dhakal K P, Duong D L, Lee J, Nam H, Kim M, Kan M, Lee Y H and Kim J 2014 Confocal absorption spectral imaging of MoS₂ *Nanoscale* **6** 13028–35
- [23] Li W *et al* 2014 Broadband optical properties of large-area monolayer CVD molybdenum disulphide *Phys. Rev. B* **90** 195434
- [24] Yim C, O'Brien M, McEvoy N, Winters S, Mirza I, Lunney J G and Duesberg G S 2014 Investigation of the optical properties of MoS₂ thin films using spectroscopic ellipsometry *Appl. Phys. Lett.* **104** 103114
- [25] Funke S, Miller B, Parzinger E, Thiesen P, Holleitner A W and Wurstbauer U 2016 Imaging spectroscopic ellipsometry of MoS₂ *J. Phys.: Condens. Matter* **28** 385301
- [26] Park J W, So H S, Kim S, Choi S-H, Lee H, Lee J, Lee C and Kim Y 2014 Optical properties of large -area ultrathin MoS₂ films: evolution from a single layer to multilayers *J. Appl. Phys.* **116** 183509
- [27] McIntyre J and Aspnes D E 1971 Differential reflection spectroscopy of very thin surface films *Surf. Sci.* **24** 417–34
- [28] Hsiang-Lin L, Shen C-C, Su S-H, Hsu C-L, Li M-Y and Li L-J 2014 Optical properties of monolayer transition metal dichalcogenides probed by spectroscopic ellipsometry *Appl. Phys. Lett.* **105** 201905
- [29] Yu Y *et al* 2015 Exciton-dominated dielectric function of atomically thin MoS₂ films *Sci. Rep.* **5** 16996
- [30] Birgina E G, Chambouleyron I E and Martínez J-E M 2003 Optimization problems in the estimation of parameters of thin films and the elimination of the influence of the substrate *J. Comput. Appl. Math.* **152** 35–50
- [31] Ishihara S *et al* 2016 Improving crystalline quality of sputtering-deposited MoS₂ thin film by postdeposition sulfurization annealing using (t-C4H9)2S2 *Japan. J. Appl. Phys.* **55** 04EJ07
- [32] Li D *et al* 2016 Optical properties of thickness-controlled MoS₂ thin films studied by spectroscopic ellipsometry *Appl. Surf. Sci.* **481** 884–890
- [33] Samassekou H, Alkabsh A, Stiwinter K, Khatri A and Mazumdar D 2018 Atomic-level insights through spectroscopic and transport measurements into the large-area synthesis of MoS₂ thin films *MRS Commun.* **8** 1328–34
- [34] Fujiwara H 2007 *Spectroscopic Ellipsometry: Principles and Applications* (Chichester: Wiley) p 81
- [35] J A Woollam Co., Inc. 1994–2012 Spectroscopic ellipsometry data acquisition and analysis software *Guid to Using WVASE* (Lincoln, NE: Woollam) p 696
- [36] Jellison G E and Modine F A 1996 Parameterization of the optical functions of amorphous materials in the interband region *Appl. Phys. Lett.* **69** 371–3
- [37] Chen H and Shen W Z 2005 Perspectives in the characteristics and applications of Tauc-Lorentz dielectric function mode *Eur. Phys. J. B* **43** 503–7
- [38] Toll J S 1956 Causality and the dispersion relation: logical foundations *Phys. Rev.* **104** 1760–70
- [39] Hu B Y 1989 Kramers–Kronig in two lines *Am. J. Phys.* **57** 821
- [40] Blaha P, Schwarz K, Madsen G K, Kvasnicka D and Luitz J 2001 WIEN2k: An Augmented Plane Wave plus Local Orbitals Program for. Calculating Crystal Properties, Karlheinz Schwarz, Techn. Universitat Wien